

# Photolysis of *n*-Propyl Formate in the Presence of O<sub>2</sub> and NO<sub>2</sub>: Peroxy Formyl Propyl Nitrate CH<sub>3</sub>CH<sub>2</sub>CH<sub>2</sub>OC(O)OONO<sub>2</sub> Synthesis and Characterization

Jesús A. Vila, Gustavo A. Argüello, and Fabio E. Malanca\*

INFIQC (CONICET), Departamento de Fisicoquímica, Facultad de Ciencias Químicas, Universidad Nacional de Córdoba, Pabellón Argentina Ala 1–2° Piso, X5000HUA Ciudad Universitaria, Córdoba, Argentina

## S Supporting Information

**ABSTRACT:** The photo-oxidation of *n*-propyl formate (initiated by chlorine atoms) was studied in the presence of NO<sub>2</sub>, and the products were identified. The Cl atom attack to the molecule occurs in four sites, leading to the formation of formic acid, carbon dioxide, dicarbonylic products, nitrates, peroxy propionyl nitrate (CH<sub>3</sub>CH<sub>2</sub>C(O)OONO<sub>2</sub>, PPN), and a new peroxy nitrate, peroxy formyl propyl nitrate (CH<sub>3</sub>CH<sub>2</sub>CH<sub>2</sub>OC(O)OONO<sub>2</sub>, PFPN). To characterize bulk quantities of the PFPN, its synthesis was carried out by the photolysis of mixtures of CH<sub>3</sub>CH<sub>2</sub>CH<sub>2</sub>OC(O)H, NO<sub>2</sub>, Cl<sub>2</sub>, and O<sub>2</sub>. After purification, its infrared spectrum and thermal stability were determined. The main infrared absorption bands and their corresponding cross sections are 796, 1219, 1302, 1741, and 1831 cm<sup>-1</sup> (1.16, 3.11, 0.88, 2.42, and 1.34 × 10<sup>-18</sup> cm<sup>2</sup> molec<sup>-1</sup>, respectively). Thermal decomposition was studied as a function of pressure from 6.0 to 1000 mbar at 298 K, and the activation energy was determined between 293 and 304 K at total pressures of 9.0 and 1000 mbar (*E*<sub>a</sub> = 98 ± 3 and 110 ± 2 kJ/mol, respectively). The atmospheric thermal lifetimes were obtained from kinetic parameters.



## INTRODUCTION

Esters are important volatile organic compounds. They are used as industrial solvents, as reagents during the manufacture of perfumes and food flavoring, and as a fumigant of stored foodstuffs due to its pesticide properties.<sup>1–4</sup> They are also emitted naturally to the atmosphere by vegetation and could be formed in the atmospheric degradation of alcohols, ethers, and new biofuels. Propyl formate (CH<sub>3</sub>CH<sub>2</sub>CH<sub>2</sub>OC(O)H) is emitted from some fruits<sup>5</sup> and is formed as a degradation product from the family of glycol ethers used in many domestic and industrial products.<sup>6</sup> Although there are not reliable estimates of the total atmospheric burden of either the formate or the peroxy nitrate itself, the latter should be considered as a potential source of pollution, and therefore, the study and understanding of its chemistry is highly needed.

Kinetic studies of reactions of formates with •OH radicals or chlorine atoms, as well as determinations of the photo-oxidation mechanisms in the presence and absence of nitrogen dioxide, have been performed by several authors who aimed to predict the possible impact of their emissions to the atmosphere. The rate coefficient for methyl, ethyl, *n*-propyl, and *n*-butyl formates with •OH radicals at 298 K (1.80 × 10<sup>-13</sup>, 8.43 × 10<sup>-13</sup>, 1.82 × 10<sup>-12</sup>, and 3.82 × 10<sup>-12</sup> cm<sup>3</sup> molec<sup>-1</sup> s<sup>-1</sup>, respectively)<sup>7</sup> show that these species can react in the troposphere, with the concomitant formation of degradation products. On the other hand, the rate coefficient of these formates with chlorine atoms has been determined by several authors.<sup>7–11</sup> The rate coefficient for *n*-propyl formate at 298 K ranges from 4.3 to 5.6 × 10<sup>-11</sup> cm<sup>3</sup> molec<sup>-1</sup> s<sup>-1</sup>.<sup>8,10</sup>

The reaction mechanism initiated by chlorine atoms in the presence and absence of NO<sub>2</sub> and the branching ratio for the attack of chlorine atoms to the different hydrogen atoms of the

molecule were determined for methyl- and ethyl formates by Wallington et al. (2001), Hansen et al. (2002), Malanca et al. (2009), and Orlando and Tyndall (2010).<sup>1,12–14</sup>

Many studies have concluded that the oxidation of either hydrogenated or fluorinated compounds in the presence of NO<sub>2</sub> leads to the formation of peroxy nitrates (ROONO<sub>2</sub>), important reservoir species in the atmosphere.<sup>15–18</sup> In particular, the photo-oxidation of formates in the presence of NO<sub>2</sub> should lead to the formation of an important family of thermally stable peroxy acyl nitrates, C<sub>x</sub>H<sub>2x+1</sub>OC(O)OONO<sub>2</sub>, of which only the shorter chain (*x* = 1, 2) congeners have been reported.<sup>1,18</sup>

In this work, we have studied the oxidation of *n*-propyl formate in the presence of NO<sub>2</sub>, determined its reaction mechanism, quantified the main products formed, and characterized the new peroxy nitrate (identified as peroxy formyl propyl nitrate CH<sub>3</sub>CH<sub>2</sub>CH<sub>2</sub>OC(O)OONO<sub>2</sub> (PFPN)), as well as determined some of its physicochemical properties.

## EXPERIMENTAL SECTION

**Materials.** Commercially available samples of propyl formate (Sigma-Aldrich), NO (AGA), and O<sub>2</sub> (AGA) were used. NO<sub>2</sub> was synthesized by the thermal decomposition of Pb(NO<sub>3</sub>)<sub>2</sub>. Cl<sub>2</sub> was prepared by the reaction between HCl and KMnO<sub>4</sub> and was then distilled.

**Procedure.** Gases were manipulated in a glass vacuum line equipped with two capacitance pressure gauges (0–760 Torr,

Received: November 18, 2015

Revised: December 22, 2015

Published: December 25, 2015

MKS Baratron; 0–70 mbar, Bell and Howell). Photolyses of mixtures of  $\text{CH}_3\text{CH}_2\text{CH}_2\text{OC}(\text{O})\text{H}$  (3.0 mbar)/ $\text{Cl}_2$  (1.5 mbar)/ $\text{NO}_2$  (0 or 0.7 mbar)/ $\text{O}_2$  (1000 mbar) were carried out in an IR gas cell (optical path 23.0 cm; silicon windows), using two black lamps, following the temporal variation of reactant and products through IR spectroscopy. Spectra were acquired in the range  $4000\text{--}400\text{ cm}^{-1}$  with a resolution of  $2\text{ cm}^{-1}$  using a Fourier transform infrared (FTIR) spectrophotometer Bruker IR IFS28. This setup was also used to quantify the products formed.

Additionally, to identify the products formed in the photo-oxidation in the absence of  $\text{NO}_2$ , samples were photolyzed in a 5 L glass flask. The resulting mixture was transferred to a set of three cold traps where its components were distilled using baths at different temperatures ( $-100$ ,  $-70$ , and  $-50\text{ }^\circ\text{C}$ ). The resulting fractions were transferred to the infrared gas cell, and their spectra were analyzed.

To characterize the PFPN, it was synthesized and further purified. The syntheses were carried out in a photoreactor maintained at low temperature ( $0\text{--}3\text{ }^\circ\text{C}$ ) to avoid its thermal decomposition. The progress of the reaction was checked every 30 min by taking small samples from the reactor and recording the infrared spectra. The photolysis was stopped when 50% of the reactant had disappeared. The resultant mixture was collected by slowly passing it through three traps kept in liquid  $\text{N}_2$  in order to remove excess  $\text{O}_2$  and noncondensable products. The distillation from  $-80$  to  $-120\text{ }^\circ\text{C}$  led to the elimination of  $\text{ClNO}$  and  $\text{CO}_2$ , and successive distillations from  $-50$  to  $-100\text{ }^\circ\text{C}$  allowed the removal of propyl formate, nitrates, and most of the formic acid. The remnant fraction contained mainly PFPN and a small amount ( $<2\%$ ) of formic acid.

Thermal stability of PFPN was determined between 293 and 304 K using a proven methodology frequently employed<sup>15,18</sup> that adds  $\text{NO}$  (1.0 mbar) to the reaction vessel in order to capture the peroxy radicals formed in the decomposition. The temporal variation of the peroxypropionyl nitrate concentration for 0.4 mbar samples of PFPN was monitored by infrared spectroscopy using the bands at  $796$  and  $1742\text{ cm}^{-1}$ . The results were analyzed according to a first-order rate law at each temperature, and thus, an Arrhenius plot was obtained.

Theoretical calculations to give the infrared spectrum were performed with the Gaussian 03 program suite.<sup>19</sup> Geometric optimizations and calculations of the vibrational frequencies of PFPN were carried out by applying density functional theory (DFT) methods, using the B3LYP exchange functional with 6-311++ G(d,p) basis.

Gas chromatography/mass spectrometry (GC/MS) analyses were performed in a Shimadzu GC-MS-QP 5050 spectrometer equipped with a capillary column Zebtron 2B-5MS ( $30\text{ m} \times 0.25\text{ mm} \times 0.25\text{ }\mu\text{m}$ ) using helium as eluent at a flow rate of 1.1 mL/min. Both injector and ion source temperatures were  $280\text{ }^\circ\text{C}$ , and the oven heating ramp was  $15\text{ }^\circ\text{C}/\text{min}$  from 25 up to  $280\text{ }^\circ\text{C}$ . The pressure in the MS instrument was  $10^{-5}$  Torr, precluding ion–molecule reactions from taking place, and MS recordings were made in the electron impact (EI) mode with ionization energy of 70 eV.

## RESULTS AND DISCUSSION

**Photo-oxidation of  $\text{CH}_3\text{CH}_2\text{CH}_2\text{OC}(\text{O})\text{H}$  in the Presence of  $\text{NO}_2$ .** Figure 1 shows the sequence of infrared spectra obtained in the photolysis of  $\text{CH}_3\text{CH}_2\text{CH}_2\text{OC}(\text{O})\text{H}$ ,  $\text{Cl}_2$ ,  $\text{NO}_2$ , and  $\text{O}_2$  mixtures. The first and second traces correspond to  $t =$

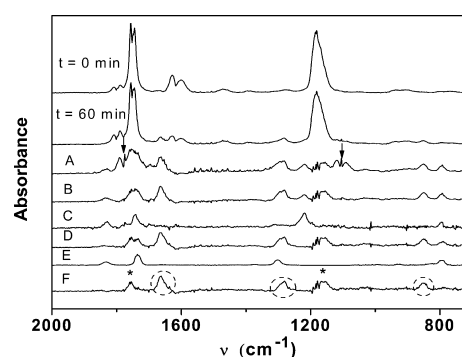


**Figure 1.** Photooxidation of *n*-propyl formate in the presence of  $\text{NO}_2$ . Traces from top to bottom: first, before irradiation; second, after 60 min photolysis; A, reaction products; B = A –  $\text{HC}(\text{O})\text{OH}$ ; C = PFPN reference spectra (see text below); D = B – PFPN; E = PPN; F = D – PPN. Arrows signal the peaks corresponding to formic acid. Circles and asterisks show the peaks corresponding to remnant nitrates and carbonyl compounds, respectively.

0 and  $t = 60$  min of irradiation, respectively. The third trace (A), obtained from the subtraction of reactants to the second one, shows the products formed. It is clear that formic acid is formed (peaks at  $1105$  and  $1775\text{ cm}^{-1}$ ). In the fourth trace (B), formic acid has been subtracted and the spectrum shows two peaks characteristic of peroxy nitrates ( $796$  and  $1742\text{ cm}^{-1}$ ). The fifth trace (C) shows the reference spectrum of PFPN, obtained as will be explained in a subsequent section. Its subtraction from the fourth trace (paying special attention to the band centered at  $1219\text{ cm}^{-1}$  that we independently know belongs to PFPN) leads to the sixth trace (D) and reveals still another peroxy nitrate formed in the photolysis. The next (seventh) trace shows the reference spectra of peroxy propionyl nitrate (PPN), whose subtraction from the sixth trace leads to the last one, in which circles highlight the formation of nitrates (bands at  $1650$ ,  $1280$ , and  $850\text{ cm}^{-1}$ ) and asterisks point to the formation of other carbonyl compounds (bands at  $1758$  and  $1166\text{ cm}^{-1}$ ). Carbon dioxide is also formed in the photolysis (although it is not shown in the figure).

Information about the identity of the carbonyl products was obtained from similar experiments carried out in the absence of nitrogen dioxide. Figure 2 shows the spectrum of products obtained in the photolysis of  $\text{CH}_3\text{CH}_2\text{CH}_2\text{OC}(\text{O})\text{H}$ ,  $\text{Cl}_2$ , and

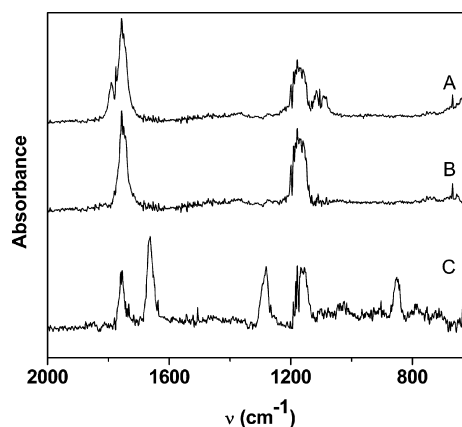
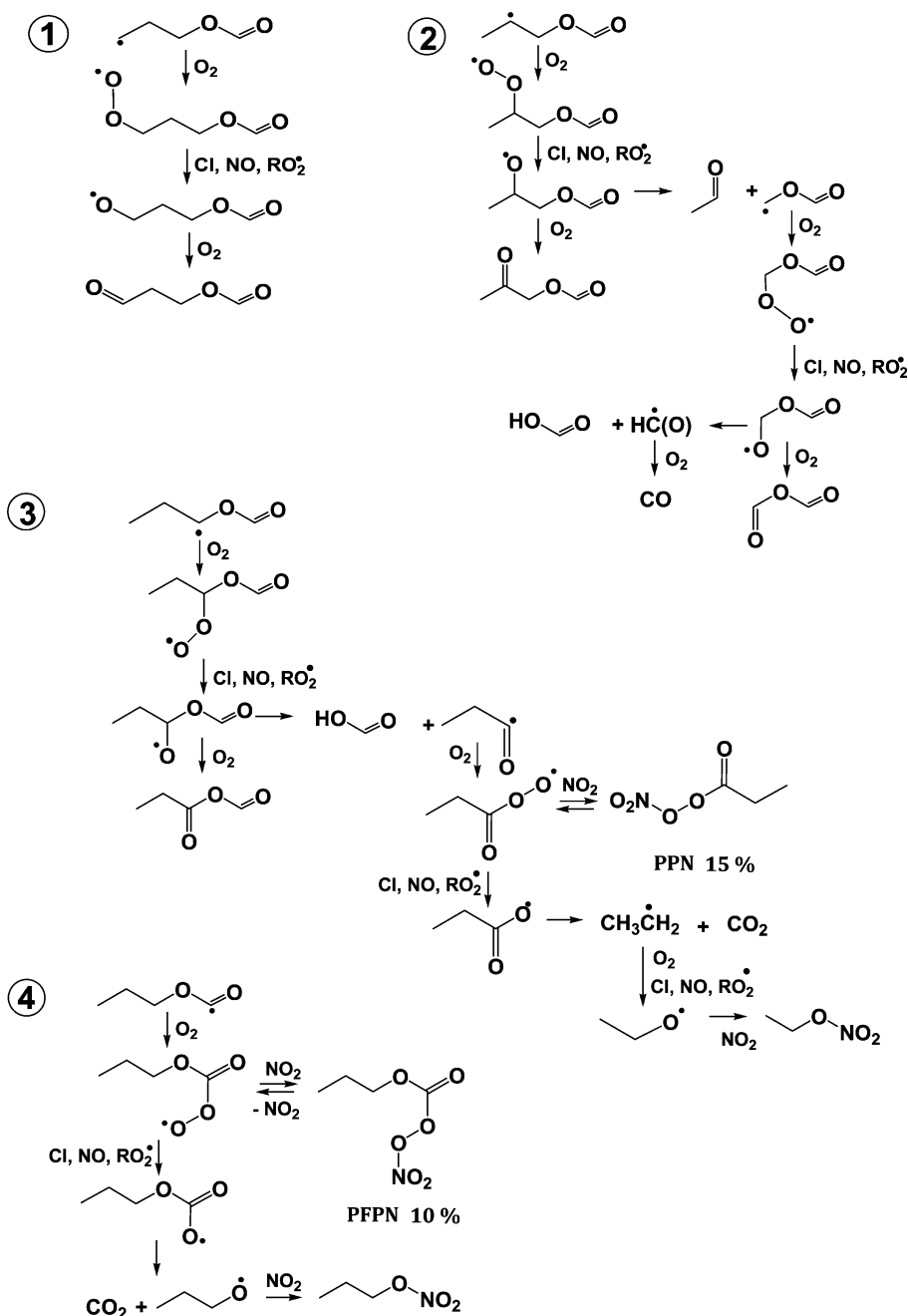


**Figure 2.** Photooxidation of *n*-propyl formate in the absence of  $\text{NO}_2$ . Traces from top to bottom: A, products after 60 min of photolysis; B = A –  $\text{HC}(\text{O})\text{OH}$ ; C, trace F taken from Figure 1 for comparison.

Scheme 1. Mechanism of Oxidation in the Presence of Nitrogen Dioxide

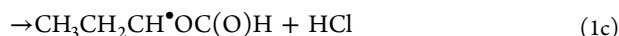
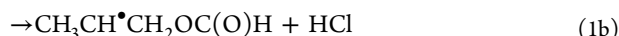
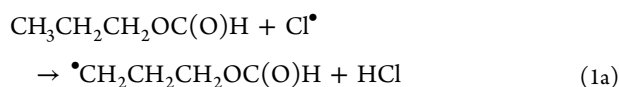


O<sub>2</sub> mixtures after 60 min of irradiation (first trace). The subtraction of a reference spectrum of formic acid to this first trace leads to a new one that shows the presence of the same carbonylic signals as those of trace F of Figure 1, although their intensities are higher in the absence of NO<sub>2</sub>. This could be explained by taking into account that the photolysis in the presence of nitrogen dioxide leads to the formation of both nitrate and peroxyxynitrate and, consequently, the formation of carbonylic products is decreased.

Identification of these carbonylic compounds required photolysis of bulk quantities in the absence of NO<sub>2</sub> and appropriate fractionation using cold baths. The most abundant products identified by FTIR were carbon dioxide and formic acid, while the less volatile fraction shows other carbonylic compounds that needed to be analyzed by gas chromatography

coupled to mass spectrometry. A typical chromatogram shows three peaks at retention times ranging from 3 to 4 min. On the basis of their fragmentation patterns, we are led to conclude that the species are CH<sub>3</sub>C(O)CH<sub>2</sub>OC(O)H (*m/e*: 15, CH<sub>3</sub><sup>+</sup>; 43, CH<sub>3</sub>CO<sup>+</sup>; 59, C<sub>3</sub>H<sub>7</sub>O<sup>+</sup>; 87, M-CH<sub>3</sub>; 101, M<sup>+</sup>), CH<sub>3</sub>CH<sub>2</sub>C(O)OC(O)H (*m/e*: 27, C<sub>2</sub>H<sub>3</sub><sup>+</sup>; 29, C<sub>2</sub>H<sub>5</sub><sup>+</sup>, CHO<sup>+</sup>; 45, CO<sub>2</sub>H<sup>+</sup>; 59, C<sub>3</sub>H<sub>7</sub>O<sup>+</sup>; 74, C<sub>3</sub>H<sub>6</sub>O<sub>2</sub><sup>+</sup>; 87, M-CH<sub>3</sub>; 101 M<sup>+</sup>), and HC(O)CH<sub>2</sub>CH<sub>2</sub>OC(O)H (29, CHO<sup>+</sup>; 44, CO<sub>2</sub><sup>+</sup>; 58, C<sub>3</sub>H<sub>6</sub>O<sup>+</sup>; 73, C<sub>3</sub>H<sub>5</sub>O<sub>2</sub><sup>+</sup>), all of them formed from the reaction of oxy radicals with molecular oxygen, as will be discussed.

The explanation of the products observed (in the presence and absence of nitrogen dioxide) could be as follows; chlorine atoms attack *n*-propyl formate at four different sites, forming the respective radicals (reactions 1a–1d)



In the presence of  $\text{O}_2$ , all of these radicals lead to the formation of peroxy radicals:  $\bullet\text{OOCH}_2\text{CH}_2\text{CH}_2\text{OC}(\text{O})\text{H}$ ,  $\text{CH}_3\text{CH}(\text{OO}^\bullet)\text{CH}_2\text{OC}(\text{O})\text{H}$ ,  $\text{CH}_3\text{CH}_2\text{CH}(\text{OO}^\bullet)\text{OC}(\text{O})\text{H}$ , and  $\text{CH}_3\text{CH}_2\text{CH}_2\text{OC}(\text{O})\text{OO}^\bullet$ . From these radicals, the only one that could lead directly to a stable peroxyxynitrate in the presence of nitrogen dioxide is the last one, which gives  $\text{CH}_3\text{CH}_2\text{CH}_2\text{OC}(\text{O})\text{OONO}_2$ . The other peroxy radicals form the oxy radicals  $\bullet\text{OCH}_2\text{CH}_2\text{CH}_2\text{OC}(\text{O})\text{H}$  (R1),  $\text{CH}_3\text{CH}(\text{O}^\bullet)\text{CH}_2\text{OC}(\text{O})\text{H}$  (R2), and  $\text{CH}_3\text{CH}_2\text{CH}(\text{O}^\bullet)\text{OC}(\text{O})\text{H}$  (R3) after interaction with either chlorine atoms or nitrogen monoxide formed from the photolysis of  $\text{NO}_2$ . These C4 alkoxy radicals still have some reaction paths available: either reaction with  $\text{O}_2$  to form dicarbonylic compounds; breaking of C–C or C–O bonds to form shorter-chain compounds;  $\alpha$ -ester rearrangement to form acids; or isomerization via a 1,5-H atom shift that preserves the length of the carbon chain.<sup>20</sup>

As might be expected by analogy to unsubstituted radicals of similar structure, reaction with  $\text{O}_2$  is a major fate for R1 to form 3-oxopropyl formate ( $\text{HC}(\text{O})\text{CH}_2\text{CH}_2\text{OC}(\text{O})\text{H}$ ), while decomposition via C–C bond cleavage appears to dominate for R2.<sup>20,21</sup> The rearrangement process could, a priori, be the major fate for R3, on account of its analogy with the  $\text{CH}_3\text{CH}(\text{O}^\bullet)\text{OC}(\text{O})\text{CH}_3$  radical, although reactions with  $\text{O}_2$ , decomposition via C–C or C–O bond scission, or isomerization may also occur to a smaller degree as pointed out by Picquet-Varrault et al. and Tuazon et al.<sup>21,22</sup> Nevertheless, R2 and R3 could still lead to minor quantities of  $\text{CH}_3\text{C}(\text{O})\text{CH}_2\text{OC}(\text{O})\text{H}$  and  $\text{CH}_3\text{CH}_2\text{C}(\text{O})\text{OC}(\text{O})\text{H}$  because of the reaction with  $\text{O}_2$ . In the presence of nitrogen dioxide, an additional path to form nitrates opens.

Scheme 1 shows the reaction mechanism in the presence of  $\text{NO}_2$ . The reactions following the formation of  $\text{CH}_3\text{CH}_2\text{CH}_2\text{OC}(\text{O})\text{OO}^\bullet$  lead to PFPN ( $\text{CH}_3\text{CH}_2\text{CH}_2\text{OC}(\text{O})\text{OONO}_2$ ). Further decomposition of PFPN could lead to  $\text{CO}_2$  and  $\text{CH}_3\text{CH}_2\text{CH}_2\text{O}^\bullet$  radicals that, in the presence of nitrogen dioxide, mainly end in *n*-propyl nitrate formation. As can be seen from the yields presented in the scheme, the formation of PFPN accounts for ~10% of the disappearance of the formate.

On the other hand, R3 leads to the formation of formic acid, PPN (15%), carbon dioxide,  $\text{CH}_3\text{CH}_2\text{C}(\text{O})\text{OC}(\text{O})\text{H}$ , and ethyl nitrate, all of them identified by infrared or mass spectroscopy. The radical R2 leads to the formation of  $\text{CH}_3\text{C}(\text{O})\text{CH}_2\text{OC}(\text{O})\text{H}$  and formic acid. Finally, the radical R1 leads to the formation of  $\text{HC}(\text{O})\text{CH}_2\text{CH}_2\text{OC}(\text{O})\text{H}$ . As expected, the quantities of formic acid formed (25%) are not modified by the addition of  $\text{NO}_2$ , considering that its formation occurs through an  $\alpha$ -ester rearrangement. The quantification of total nitrates formed in the photolysis with  $\text{NO}_2$  explains about  $(26 \pm 3)\%$  of the disappearance of the precursor formate.

**Infrared Spectrum of PFPN.** Figure 3 shows the experimental and calculated spectra of PFPN as well as the infrared absorption cross sections. There is a good concordance between both spectra. This feature could also be used as a

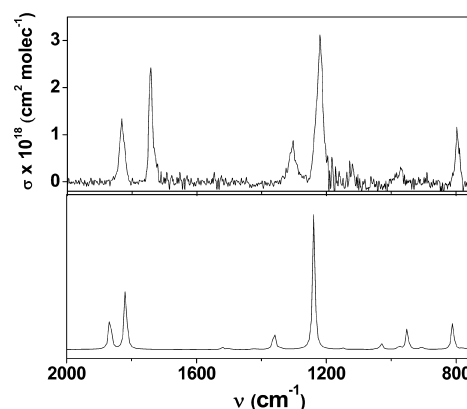


Figure 3. Absorption cross sections and calculated spectra of PFPN.

confirmation corroborating the identity of PFPN. The calculated spectrum was obtained from the most stable conformer syn–syn (Figure 4), derived by structure

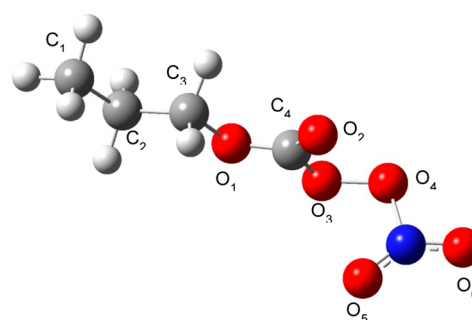


Figure 4. Calculated structure for the most stable conformer (syn–syn conformer).

optimization (see below). The calculation of the vibrational frequencies of possible conformers of PFPN were carried out by applying density functional theory (B3LYP) methods with 6-311++ G(d,p) basis sets.

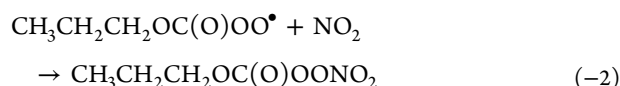
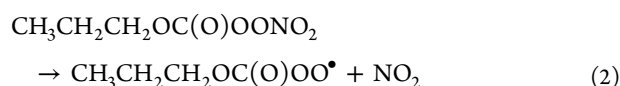
During the optimization process of the possible conformers, some common features, regardless of the starting structure, were observed:

- The dihedral angle formed by the fragment H(1,2,3)–C1–C2–C3 adopts the configuration “anti” ( $180^\circ$ ) as well as the other dihedrals formed with the fragments C1–C2–C3–O1 and C2–C3–O1–C4.
- The dihedral angle formed by the fragment O3–O4–N1–O5 adopts the configuration “syn” (close to  $0^\circ$ ) similar to other peroxyxynitrates.<sup>23</sup>

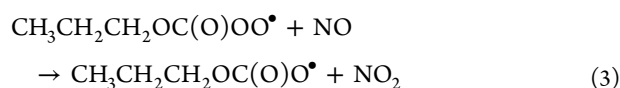
Therefore, by setting fixed values for these dihedral angles, the study focused on the remaining ones, which define the position of the C=O bond with respect to the peroxidic bond O3–O4. The conformers were named according to the following criteria: (a) the position of the C=O bond with respect to the O–O bond defines the first term, whether syn or anti; and (b) the position of the  $\text{CH}_3\text{CH}_2\text{CH}_2\text{—O}$  bond with respect to the C=O bond defines the second syn–anti term. The calculations reveal that the most stable conformer is syn–syn, in accordance with results obtained for  $\text{CH}_3\text{CH}_2\text{OC}(\text{O})\text{OONO}_2$  by Bossolasco et al. (2011).<sup>18</sup> Tables S1 and S2 show the calculated geometric parameters and Cartesian coordinates. The calculated values for both the dihedral (C–O–O–N) and

the O–O bond distance agree with the literature values.<sup>14,18,19,24</sup>

**Thermal Decomposition of CH<sub>3</sub>CH<sub>2</sub>CH<sub>2</sub>OC(O)OONO<sub>2</sub>.** PFPN exists in equilibrium with NO<sub>2</sub> and CH<sub>3</sub>CH<sub>2</sub>CH<sub>2</sub>OC(O)OO• radicals



To measure the rate coefficient for the thermal decomposition, the presence of a radical scavenger is needed. Nitrogen monoxide was added because it efficiently removes the CH<sub>3</sub>CH<sub>2</sub>CH<sub>2</sub>OC(O)OO• radicals because of the occurrence of the following reactions (reactions 3–6), thus avoiding the regeneration of PFPN (reaction –2):



The temporal variation of the peroxy nitrates concentration was followed by FTIR as was described previously, and the rate coefficient measured ( $k_{\text{obs}}$ ) was corrected using the following equation,

$$k_2 = k_{\text{obs}} \left( 1 + \frac{k_{-2}[\text{NO}_2]}{k_3[\text{NO}]} \right)$$

which takes into account that, during the thermal decomposition, the nitrogen dioxide concentration increases. The rate coefficients for reactions –2 and 3 were taken from literature values corresponding to similar radicals, as has been done by many authors ( $k_{-2} = 1.12 \times 10^{-11}$ ,  $k_3 = 2.11 \times 10^{-11}$  cm<sup>3</sup> molecule<sup>-1</sup> s<sup>-1</sup>).<sup>25,26</sup> Nevertheless, this correction accounts for 6% of  $k_{\text{obs}}$  at most. This percentage arises from the use of the reported rate coefficients for reactions –2 and 3 as well as the experimental concentration for nitrogen monoxide added to the system and the maximum nitrogen dioxide concentration formed as a consequence of PFPN decomposition.

To establish the dependence of the rate coefficient of reaction 2 with pressure, a series of experimental runs were performed at 298 K at different total pressures. The results presented in Figure 5 show that the dependence is similar to that reported by Bossolasco et al. (2011)<sup>18</sup> for peroxy ethoxy formyl nitrate (PEFN), although we cannot explain why the high-pressure limit has not been reached at 1000 mbar for a molecule possessing a higher number of degrees of freedom.

The kinetic parameters ( $E_a$ , activation energy, and  $A$ , pre-exponential factor) derived from the figure give the following values at 9.0 and 1000 mbar:  $E_a = (98 \pm 3)$  kJ/mol and  $\ln A = (31 \pm 1)$ ;  $E_a = (110 \pm 2)$  kJ/mol and  $\ln A = (36.1 \pm 0.8)$ , respectively. The comparison of the values of  $E_a$  determined at 1000 mbar with those reported for CH<sub>3</sub>OC(O)OONO<sub>2</sub> (107 ± 5 kJ/mol)<sup>27</sup> and C<sub>2</sub>H<sub>5</sub>OC(O)OONO<sub>2</sub> (108 ± 5 kJ/mol)<sup>18</sup> shows good agreement for the family C<sub>x</sub>H<sub>2x+1</sub>OC(O)OONO<sub>2</sub>.

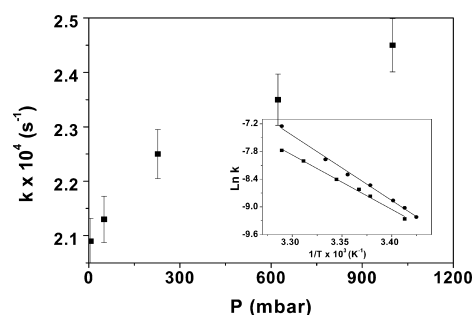


**Figure 5.** Thermal decomposition of PFPN as a function of pressure. Errors bars represent one standard deviation taken from the temporal variation of peroxy nitrates at each pressure.

The closeness of the values for  $E_a$ , all of them comprised within the experimental errors, preclude us to establish a definite trend in the stability of this family as a function of the length of the carbonated chain.

## CONCLUSIONS

In this paper, we determined the main products resulting from the photo-oxidation of *n*-propyl formate, in both the presence and the absence of NO<sub>2</sub>, as well as the reaction mechanism. In the atmosphere, emissions of *n*-propyl formate could contribute to the formation of nitrates, dicarbonyl compounds, and PFPN.

The comparison of its thermal stability with peroxy nitrates of shorter carbonated chains C<sub>x</sub>H<sub>2x+1</sub>OC(O)OONO<sub>2</sub> ( $x = 2, 3$ ) leads one to conclude that this family could act as a reservoir species in the atmosphere. In particular, the lifetime of PFPN at an altitude of 2 km is ~1 day. It rapidly increases up to 7 months at 6 km, reaching values of years near the tropopause.

## ASSOCIATED CONTENT

### Supporting Information

The Supporting Information is available free of charge on the ACS Publications website at DOI: 10.1021/acs.jpca.5b11313.

Geometric parameters for the syn–syn PFPN conformer (Table S1) and Cartesian matrix for syn–syn PFPN (Table S2) (PDF)

## AUTHOR INFORMATION

### Corresponding Author

\*E-mail: fmalanca@fcq.unc.edu.ar.

### Notes

The authors declare no competing financial interest.

## ACKNOWLEDGMENTS

Financial support from SECYT-Universidad Nacional de Córdoba, ANPCyT, and CONICET is gratefully acknowledged. J.A.V. acknowledges the fellowship he holds from CONICET.

## REFERENCES

- (1) Wallington, T. J.; Hurley, M. D.; Maurer, T.; Barnes, I.; Becker, K. H.; Tyndall, G. S.; Orlando, J. J.; Pimentel, A. S.; Bilde, M. Atmospheric Oxidation Mechanism of Methyl Formate. *J. Phys. Chem. A* **2001**, *105*, 5146–5154.
- (2) Cavalli, F.; Barnes, I.; Becker, K. H.; Wallington, T. J. Atmospheric Oxidation Mechanism of Methyl Propionate. *J. Phys. Chem. A* **2000**, *104*, 11310–11317.

- (3) Simmons, P.; Fisher, C. K. Ethyl Formate and Isopropyl Formate as Fumigants for Packages of Dried Fruits. *J. Econ. Entomol.* **1945**, *38*, 715–716.
- (4) Cotton, R. T. *Fumigating Stored Foodstuffs, Yearbook of Agriculture*; U.S. Government Printing Office: 1952; pp 345–349.
- (5) Yahia, E. M. Apple Flavor. *Hortic. Rev.* **2010**, *16*, 197–233.
- (6) Markgraf, S. J.; Semple, J.; Wells, J. R. The Hydroxyl Radical Reaction Rate Constant and Atmospheric Transformation Products of 2-Propoxyethanol. *Int. J. Chem. Kinet.* **1999**, *31*, 315–322.
- (7) Le Calve, S.; Le Bras, G.; Mellouki, A. Temperature Dependence for the Rate Coefficients of the Reactions of the OH Radical with a Series of Formates. *J. Phys. Chem. A* **1997**, *101*, 5489–5493.
- (8) Notario, A.; Le Bras, G.; Mellouki, A. Absolute Rate Constants for the Reactions of Cl Atoms with a Series of Esters. *J. Phys. Chem. A* **1998**, *102*, 3112–3117.
- (9) Good, D. A.; Hansen, J.; Kamoboures, M.; Santiono, R.; Francisco, J. S. An Experimental and Computational Study of the Kinetics and Mechanism of the Reaction of Methyl Formate with Cl Atoms. *J. Phys. Chem. A* **2000**, *104*, 1505–1511.
- (10) Wallington, T. J.; Hurley, M. D.; Haryanto, A. Kinetics of the Gas Phase Reactions of Chlorine Atoms with a Series of Formates. *Chem. Phys. Lett.* **2006**, *432*, 57–61.
- (11) Bravo, I.; Aranda, A.; Díaz-de-Mera, Y.; Moreno, E.; Tucceri, M. E.; Rodríguez, D. Kinetics, Mechanistic and Temperature Dependence Study of the Cl Reactions with  $\text{CH}_3\text{OC}(\text{O})\text{H}$  and  $\text{CH}_3\text{CH}_2\text{OC}(\text{O})\text{H}$ : Atmospheric Implications. *Phys. Chem. Chem. Phys.* **2009**, *11*, 384–390.
- (12) Hansen, J. C.; Francisco, J. S.; Szenté, J. J.; Maricq, M. M. An Experimental Study of the Mechanism and Branching Ratio for the Reaction Between Methyl Formate and Chlorine Atoms. *Chem. Phys. Lett.* **2002**, *365*, 267–278.
- (13) Malanca, F. E.; Fraire, J. C.; Argüello, G. A. Kinetics and Reaction Mechanism in the Oxidation of Ethyl Formate in the Presence of  $\text{NO}_2$ . Atmospheric implications. *J. Photochem. Photobiol., A* **2009**, *204*, 75–81.
- (14) Orlando, J. J.; Tyndall, G. S. The Atmospheric Oxidation of Ethyl Formate and Ethyl Acetate over a Range of Temperatures and Oxygen Partial Pressures. *Int. J. Chem. Kinet.* **2010**, *42*, 397–413.
- (15) Kirchner, F.; Thuner, L. P.; Barnes, I.; Becker, K. H.; Donner, B.; Zabel, F. Thermal Lifetimes of Peroxynitrates Occurring in the Atmospheric Degradation of Oxygenated Fuel Additives. *Environ. Sci. Technol.* **1997**, *31*, 1801–1804.
- (16) von Ahsen, S.; García, P.; Willner, H.; Argüello, G. A. Trifluoromethoxycarbonyl Peroxynitrate,  $\text{CF}_3\text{OC}(\text{O})\text{OONO}_2$ . *Inorg. Chem.* **2005**, *44*, 5713–5718.
- (17) Manetti, M. D.; Malanca, F. E.; Argüello, G. A. Thermal Decomposition of Trifluoromethoxycarbonyl Peroxy Nitrate,  $\text{CF}_3\text{OC}(\text{O})\text{O}_2\text{NO}_2$ . *Int. J. Chem. Kinet.* **2008**, *40*, 831–838.
- (18) Bossolasco, A. G.; Malanca, F. E.; Argüello, G. A. Peroxy ethoxyformyl nitrate,  $\text{CH}_3\text{CH}_2\text{OC}(\text{O})\text{OONO}_2$ . Spectroscopic and Thermal Characterization. *J. Photochem. Photobiol., A* **2011**, *221*, 58–63.
- (19) Frisch, M. J.; Trucks, G. W.; Schlegel, H. B.; Scuseria, G. E.; Robb, M. A.; Cheeseman, J. R.; Zakrzewski, V. G.; Montgomery, J. A., Jr.; Stratmann, R. E.; Burant, J. C.; et al. *Gaussian 98, Revision A.7*; Gaussian, Inc.: Pittsburgh, PA, 1998.
- (20) Orlando, J. J.; Tyndall, G. S.; Wallington, T. J. The Atmospheric Chemistry of Alkoxy Radicals. *Chem. Rev.* **2003**, *103*, 4657–4689.
- (21) Picquet-Varrault, B.; Doussin, J.-F.; Durand-Jolibois, R.; Carlier, P. FTIR Spectroscopic Study of the OH-induced Oxidation of two Linear Acetates: Ethyl and n-propyl Acetate. *Phys. Chem. Chem. Phys.* **2001**, *3*, 2595–2606.
- (22) Tuazon, E. C.; Aschmann, S. M.; Atkinson, R.; Carter, W. P. L. The Reactions of Selected Acetates with the OH Radical in the Presence of NO: Novel Rearrangement of Alkoxy Radicals of Structure  $\text{RCO}_2\text{CO}^*\text{R}'$ . *J. Phys. Chem. A* **1998**, *102*, 2316–2321.
- (23) Kopitzky, R.; Willner, H.; Mack, H. G.; Pfeiffer, A.; Oberhammer, H. IR and UV Absorption Cross Sections, Vibrational Analysis and the Molecular Structure of Trifluoromethyl Peroxynitrate  $\text{CF}_3\text{OONO}_2$ . *Inorg. Chem.* **1998**, *37*, 6208–6213.
- (24) Badenes, M. P.; Cobos, J. C. Quantum Chemical Study of the Atmospheric  $\text{C}_2\text{H}_5\text{C}(\text{O})\text{OONO}_2$  (PPN) Molecule and of the  $\text{C}_2\text{H}_5\text{C}(\text{O})\text{OO}$  and  $\text{C}_2\text{H}_5\text{C}(\text{O})\text{O}$  Radicals. *J. Mol. Struct.: THEOCHEM* **2008**, *856*, 59–70.
- (25) Froyd, K. D.; Lovejoy, E. R. Direct Measurement of the  $\text{C}_2\text{H}_5\text{C}(\text{O})\text{O}_2 + \text{NO}$  Reaction Rate Coefficient Using Chemical Ionization Mass Spectrometry. *Int. J. Chem. Kinet.* **1999**, *31*, 221–228.
- (26) Kerr, J. A.; Stocker, D. W. The Kinetics and Mechanism of the Photooxidation of Propionaldehyde Under Simulated Atmospheric Conditions. *J. Photochem.* **1985**, *28*, 475–489.
- (27) Kirchner, F.; Mayer-Figge, A.; Zabel, F.; Becker, K. H. Thermal Stability of Peroxynitrates. *Int. J. Chem. Kinet.* **1999**, *31*, 127–144.